Available online at www.sciencedirect.com
ScienceDirect
Journal of Hazardous Materials 153 (2008) 1149–1156
Journal of Hazardous Materials
www.elsevier.com/locate/jhazmat

Sorption of reactive dye from aqueous solution on biomass fly ash

P. Pengthamkeerati *, T. Satapanajaru, O. Singchan

Department of Environmental Science, Faculty of Science, Kasetsart University, Bangkok 10900, Thailand

Received 5 June 2007; received in revised form 21 August 2007; accepted 20 September 2007
Available online 29 September 2007

Abstract

This study investigates the adsorption behavior of Reactive Black 5 (RB) and Reactive Yellow 176 (RY) from aqueous solution on coal fly ash (FA-CO), HCl-treated coal fly ash (TFA-HCl), and biomass fly ash (FA-BM). In preliminary study, the FA-BM showed the greatest dye adsorption capacity of both dyes, compared to FA-CO and TFA-HCl. Hence only for the FA-BM, the effects of various experiment parameters (e.g. solution pH, ionic strength, initial dye concentration, contact time) were spectrophotometrically determined. At the final pH of 8.1–8.5, the adsorption capacity of both dyes on the FA-BM was maximum and decreased above or below this pH. A positive effect of salt addition on the dye adsorption capacity was observed. The adsorption capacity of dye on the FA-BM increased with increasing C_0. The equilibrium data of both dyes on the FA-BM were fitted to both Langmuir and Freundlich isotherms, but the experimental data of the RB was found to be little better fitted by the Langmuir model. The sorption data was good fit with the pseudo-second-order kinetic model. These results indicate that biomass fly ash is an interesting alternative for dye removal from the wastewater.

Keywords: Fly ash; Reactive dyes; Adsorption isotherm; First-order kinetic model; Pseudo-second-order kinetic model

1. Introduction

Synthetic dye has been increasingly used in textile industry [1–4]. The textile wastewaters exhibit high color and other substances [5]. Without appropriate treatment, discharge of dye wastewaters into water bodies can adversely affect aquatic environment by reducing light penetration and photosynthesis, and being hazardous and toxic to aquatic life [3,4,6,7]. Conventional methods for treating dye wastewater, e.g. coagulation/flocculation, chemical oxidation, activated sludge process, are difficult, ineffective or economic disadvantage [2–4,6,8–10]. Adsorption is an attractive and effective method for dye removal from wastewater, especially if the adsorbent is cheap and widely available [5,7,11–14]. Many low-cost adsorbents have been investigated on dye removal, such as fly ash [3,5,12,14,15], bottom ash [7], clay [8], zeolite [1,8], calcine alunite [16], peanut hull [2], rice husk [4], and brown seaweed [10].

Biomass has long been used in the boiler for energy production [17]. Various kinds of plant biomass commonly used for this purpose include trees, trims, sawdust, wheat straw, and rice husks. After biomass combustion, a waste called fly ash is produced and needed appropriate disposal. This ash is increasingly produced and available in large quantities [3]. Since biomass fly ash is enriched with SiO_2 and contained a portion of unburned carbon, this waste has been previously used as adsorbent to removal hazardous substances from the environment, in particular from wastewater [3,18]. Therefore, this waste can be a potentially low-cost adsorbent for wastewater treatment. Combustion of biomass has a specific recipe to give sufficient energy. In common, combustion recipe uses various kinds of biomass. Hence, there is of interest to investigate the sorption behavior of mixed biomass fly ash.

While a number of investigations have been reported on fly ash for dye adsorption, more information is still needed for better understanding in the difference in dye adsorption by different fly ashes. Adsorption capacity depends on the properties of adsorbents, such as porous structure, chemical structure, and surface area [7,9]. Therefore, this study investigated the effect of fly-ash properties on dye adsorption. Selected fly ashes with different

* Corresponding author. Tel.: +662 942 8036; fax: +662 942 8715.
E-mail address: fsciptp@ku.ac.th (P. Pengthamkeerati).

0304-3894/$ – see front matter © 2007 Elsevier B.V. All rights reserved.
doi:10.1016/j.jhazmat.2007.09.074

properties used in this study are biomass fly ash, coal fly ash, and HCl-treated coal fly ash. Coal fly ash has a similar major chemical composition to the treated coal fly ash, but much less surface area. Biomass fly ash is different from coal and treated coal fly ashes for both major chemical composition and surface area.

Fly ash with the best adsorption capacity of dye was chosen for further investigation. The effects of pH, ionic strength, initial dye concentration, and contact time on dye adsorption by the fly ash were examined using batch experiment.

2. Materials and methods

2.1. Materials and characterization

The biomass fly ash (FA-BM) used in this study was obtained from the electric power plant in the eastern part of Thailand. The FA-BM was produced from combustion of biomass, mainly composed of Eucalyptus trims and chips and rice husks. The sample was oven-dried at 70 °C for 24 h and kept in a desiccator for further analysis.

The coal fly ash (FA-CO) was supplied by the Mae-Moh electric power station in the northern part of Thailand. The FA-CO was produced from lignite coal. The sample was oven-dried at 105 °C for 24 h before use. The FA-CO was treated in 1M HCl at a solution to fly-ash ratio of 10:1 by weight. The mixture was then incubated at 100 °C for 24 h. At the end of the treatment, the mixture was filtered, washed thoroughly, and oven-dried at 105 °C for 24 h. The FA-CO and HCl-treated coal fly ash (TFA-HCl) were then subjected to further analysis.

Particle size distribution of the studied fly-ash samples was determined by sieving the samples manually shaking with stainless steel mesh screens with openings of standard 53, 125, 180, and 425 μm ASTM sieves (Table 1). Specific surface area (SSA) was analyzed by Autosorb-1 analyzer using BET method and chemical composition of the samples was determined by X-ray fluorescence (XRF) analyzer (Table 2). Loss on ignition (LOI) was determined by combusting the samples at 850 °C for 1 h. Scanning electron microscopy (SEM) and pH of point of zero charge (pH_{pzc}) using the pH drift method [13] were performed on the selected samples.

The dyes used in this study were Reactive Black 5 (RB) and Reactive Yellow 176 (RY), obtained from a textile company in Thailand. These dyes are azo and contain anionic sulphonate groups. Only chemical structure of RB is made available by the supplier (Fig. 1) [6]. Natural pH of RB is 5.8.

Table 1
Particle size distribution of biomass fly ash (FA-BM) and coal fly ash (FA-CO)

Particle diameter (μm)	% Weight	
	FA-BM	FA-CO
<53	22.0	70.5
53–125	30.5	20.5
125–180	16.7	5.9
180–425	26.1	2.9
>425	4.7	0.2

Table 2
Chemical composition and specific surface area of biomass fly ash (FA-BM), coal fly ash (FA-CO), and HCl-treated coal fly ash (TFA-HCl)

Constituent	% Weight		
	FA-BM	FA-CO	TFA-HCl
SiO_2	91.05	45.84	60.90
Al_2O_3	ND[a]	13.62	19.43
CaO	1.04	9.68	4.42
Fe_2O_3	0.14	6.74	7.03
K_2O	0.95	1.55	1.96
MgO	0.14	0.38	1.10
SO_3	0.13	21.18	0.39
Loss on ignition (LOI)	5.86	0.40	3.87
Specific surface area ($m^2\ g^{-1}$)	14.32	3.39	61.84

[a] ND is not detected.

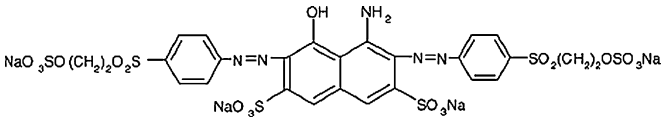

Fig. 1. Chemical structure of RB.

2.2. Adsorption study

Batch experiment was carried out to measure the adsorption characteristics of dyes by the fly ashes. The fly ash (2 g) was added to 40 ml of synthetic dye solutions of varying concentration (10–500 mg l^{-1}). Two identical mixtures were shaken on orbital shaker at 130 rpm for various times to determine the equilibrium time at room temperature and for 24 h for other experiments. After shaking, the mixture was filtered and the supernatant was measured the final pH using pH meter (EcoScan pH6 model) and the remaining dye using UV–vis spectrophotometer (GBC UV/VIS model) at λ_{max} of 598 and 400 nm for the RB and RY, respectively. To understand the adsorption behavior of dye on fly-ash surface, the fly-ash samples after performing dye adsorption were oven-dried at 70 °C for 48 h for SEM analysis.

Preliminary study was performed to determine the fly ash with the highest dye adsorption capacity. This fly ash was then selected for the following studies. The effect of solution pH was investigated by performing the adsorption experiments at various pH levels (2–12) adjusting by diluted HCl or NaOH solution. The effect of ionic strength on adsorption of dyes was tested by addition of NaCl to the solution. The concentration of NaCl used ranged from 0 to 20 mg l^{-1}. Langmuir and Freundlich isotherms were applied to determine the adsorption capacity of the fly ash. Kinetic models were used to examine the controlling mechanism of adsorption processes.

3. Results and discussion

3.1. Comparison of dye adsorption capacity by all the studied fly ashes

Property of fly ash plays a significant role in dye adsorption capacity. Fig. 2a showed dye adsorption capacity of the stud-

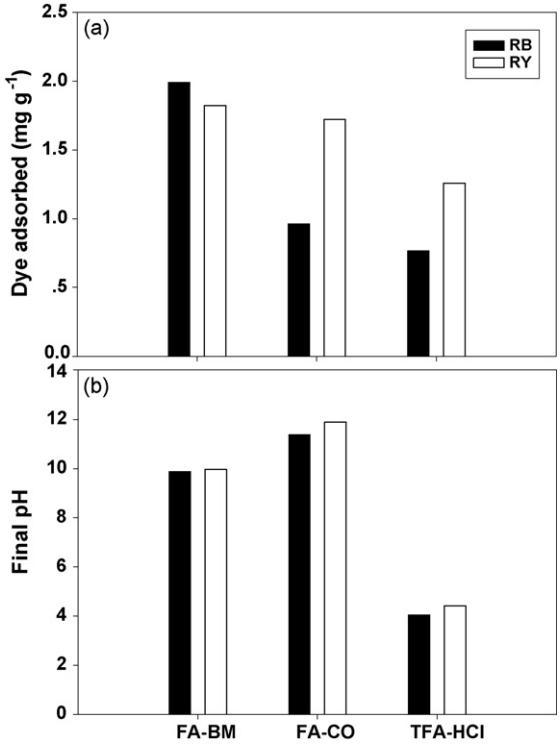

Fig. 2. Dye adsorption capacity (a) and final pH (b) of RB and RY on the studied fly ashes. Experimental conditions: initial dye concentration, 100 mg l^{-1}; fly-ash dose, 2 g/40 ml; contact time, 24 h.

ied fly ashes, and Fig. 2b showed the final pH of solution after performing dye adsorption. For both RB and RY, the FA-BM had a highest dye adsorption capacity, compared to the FA-CO and TFA-HCl. The RY tended to be greater adsorbed on the FA-CO and TFA-HCl than the RB, but was similar for the FA-BM. After dye adsorption, the final pH was about 10, 12, and 4 for the FA-BM, FA-CO, and TFA-HCl.

The different dye adsorption capacity by the studied fly ashes can be attributed to different fly-ash property. For example, different chemical composition among the FA-BM, FA-CO, and TFA-CO may influence dye adsorption. FA-BM was mainly composed of SiO_2 and unburned carbon (assumed from LOI), while the FA-CO and TFA-HCl contained similar major components of SiO_2, Al_2O_3, and Fe_2O_3 (Table 2). pH_{pzc} is the pH at which the net surface charge on adsorbent is zero. The adsorbent surface has a net positive charge at $pH < pH_{pzc}$, while has net negative charge at $pH > pH_{pzc}$ [5,13,14,19]. The pH_{pzc} of SiO_2, α-Al_2O_3, and α-Fe_2O_3 was 2, 9.1, and 6.7, respectively [20]. Because the final pH of FA-BM in the solution was about 10, the surface of SiO_2 was net negatively charged and dyes were also negatively charged (e.g., natural pH of RB = 5.8), indicating the repulsive electrostatic force between SiO_2 and dyes. In addition, this final pH was greater than the pH_{pzc} of FA-BM, which was 8.7 (Fig. 3), also suggesting the electrostatic repulsion between net negative charged FA-BM and dyes. Based on this information, the dye adsorption of FA-BM should be low. However in this study, FA-BM had a relatively high dye adsorption capacity, suggesting that there were other mechanisms than the electrostatic mechanism for dye adsorption. We suspected that the dye

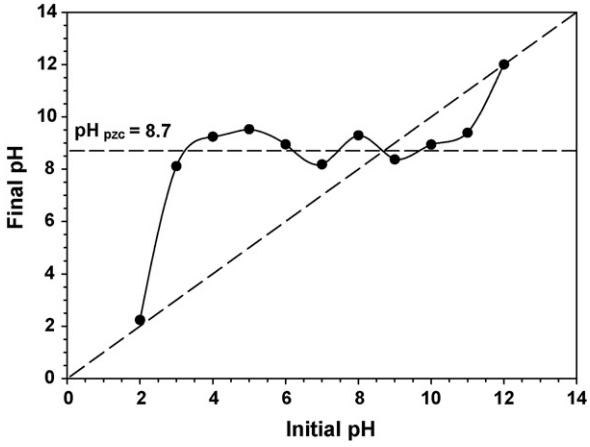

Fig. 3. Determination of pH_{pzc} of the FA-BM.

adsorption capacity of FA-BM may partly be attributed to the influence of unburned carbon. Al-Degs et al. [19] suggested the other interactions between activated carbon and dye molecules were hydrogen bonding and hydrophobic–hydrophobic mechanisms.

At highly basic condition of FA-CO (the final pH of about 12), all the major chemical components (SiO_2, Al_2O_3, and Fe_2O_3) and dyes were net negatively charged, causing the electrostatic repulsion between dye and FA-CO. Therefore, the dye adsorption capacity of FA-CO was relatively low, especially for the RB. At acidic condition of TFA-HCl (the final pH of about 4), SiO_2 in the TFA-HCl was negatively charged and dye molecules were neutral or partially positively charged, causing the electrostatic attraction. However, at this acidic pH, the positively-charged Al_2O_3 and Fe_2O_3 in the TFA-HCl reduced the degree of positive charges of SiO_2. As a result, the dye adsorption capacity of TFA-HCl was not high. In this study, the dye adsorption capacity of the TFA-HCl was not well explained by SSA. This was because TFA-HCl had the highest SSA, but presented the lowest adsorption capacity (Table 2).

Due to the highest dye adsorption capacity among all the studied fly ashes, the FA-BM was chosen for further investigation.

3.2. *Effect of solution pH*

Solution pH is an important factor controlling the surface charge of the adsorbent and the degree of ionization of the materials in the solution [3]. Fig. 4 showed the relationship between final pH and dye adsorption capacity of the FA-BM. The adsorption patterns of both RB and RY were similar in the studied pH range. The adsorption capacity increased when the final pH was increased from 2.5 to 8.5 for the RB and from 5.3 to 8.1 for the RY. After these pH ranges, the adsorption capacity of the RB slightly decreased, while the decreased adsorption was greater for the RY.

The pH effect on dye adsorption observed in this study was explained by electrostatic interaction between FA-BM and dye molecules. Maximum dye adsorption was observed in the pH range of 8.1–8.5. In this pH range, the surface of FA-BM was

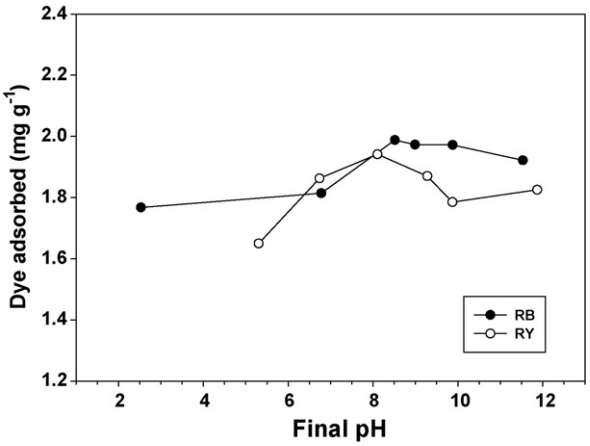

Fig. 4. Relationship between the final pH and dye adsorption capacity of RB and RY on biomass fly ash. Experimental conditions: initial dye concentration 100 g l^{-1}; fly-ash dose 2 g/40 ml; contact time 24 h.

positively charged (pH_{pzc} = 8.7) and dye was negatively charged (e.g., deprotonate sulphonate groups ($-SO_3^-$)), indicating the electrostatic attraction between the FA-BM and dye molecules. Since the studied dyes were weak acids, these dyes dissociated less towards an acidic pH. Hence, at acidic pH, the adsorption capacity decreased due to the electrostatic repulsion between the positive charged FA-BM and the neutral ($-SO_3H$) or partially positive charges of dye. At pH > pH_{pzc}, the decreased dye adsorption capacity of FA-BM was attributed to the repulsive interaction between the negatively charged FA-BM and the deprotonated dye molecules. However for the RB, the dye adsorption capacity was constant in the pH range of 8.5–10, suggesting that dye adsorption was influenced not only by electrostatic forces, as was mentioned in the Section 3.1. Al-Degs et al. [19] also observed a similar constant dye adsorption capacity over a pH range of 4–8, indicating the interaction between activated carbon and dye molecules via hydrogen-bonding and hydrophobic–hydrophobic forces.

3.3. Effect of ionic strength

The adsorption of dyes on the FA-BM was slightly positively affected by the presence of NaCl (Fig. 5). Interestingly, increasing NaCl concentration enhanced dye adsorption capacity of the FA-BM. The effect of NaCl was more pronounced for the RY than the RB. In theory, increasing ion strength will decrease adsorption capacity when there is the electrostatic attraction between the adsorbent surface and adsorbate ions [19]. But increasing ion strength will increase adsorption capacity when the electrostatic force is repulsive. In this study, the increasing adsorption capacity with the ionic strength was in agreement with this assumption. Since the final pH > pH_{pzc}, there was the electrostatic repulsion between the negatively charged FA-BM and the deprotonated dye molecules. In Fig. 5, the final pH decreased towards the pH_{pzc} of FA-BM with an increase in ionic strength, indicating less repulsive interaction between the FA-BM and dye. Therefore, dye adsorption was increased with ionic strength.

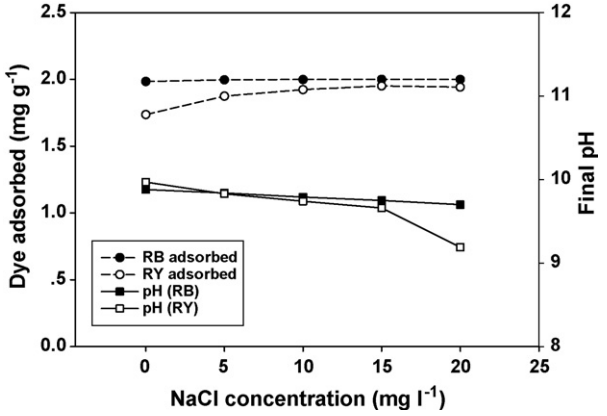

Fig. 5. The effect of ionic strength on dye adsorption capacity of RB and RY by biomass fly ash and the final pH of solution. Experimental conditions: initial dye concentration, 100 mg l^{-1}; fly ash dose, 2 g/40 ml; contact time, 24 h.

In addition, an increase in dye adsorption with increasing ionic strength may be due to an increase in dimerization of reactive dye in solution [19]. Dimerization of dye molecules was induced by salt ions, which subsequently increased dye adsorption on the adsorbent surface. Dimerization of dye was explained by intermolecular forces, including van der Waals force, ion–dipole force, and dipole–dipole force, which increased with salt concentration [19]. Janos et al. [5] and Al-Degs et al. [19] also found positive or no effect of ionic strength on dye adsorption by activated carbon and coal fly ash, respectively. The information on no salt effect on dye adsorption by fly ash is of interest for potential applications to real wastewater [5].

3.4. Effect of initial dye concentration

Fig. 6 showed the effect of initial dye concentration (C_0) (10–500 mg l^{-1}) on the adsorption capacity and removal efficiency by the FA-BM. The adsorption capacity increased from 0.2 to 4.34 and from 0.20 to 3.85 mg g^{-1} with increasing C_0 of the RB and RY, respectively. The effect of C_0 observed in this

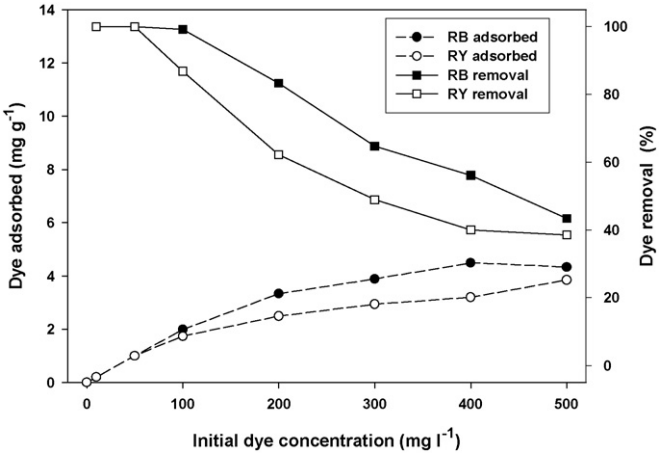

Fig. 6. The effect of initial dye concentration on dye adsorption capacity and removal efficiency of RB and RY by biomass fly ash. Experimental conditions: fly-ash dose, 2 g/40 ml; contact time, 24 h.

study suggests that the increase in C_0 enhances the interaction between dye and FA-BM. In another word, C_0 is a driving force to overcome the resistances to the mass transfer of dye between the solution and the adsorbent surface [3]. Only for the RB, the adsorption capacity beyond $C_0 = 400\,\mathrm{mg\,l^{-1}}$ did not increase, suggesting that the fly ash reached its maximum adsorption capacity [4].

3.5. Sorption isotherm

The data obtained from the equilibrium studies were analyzed using Langmuir and Freundlich adsorption isotherms. The Langmuir isotherm was given by the following equation.

$$\frac{C_e}{q_e} = \frac{1}{(Q_0 K_L)} + \left(\frac{1}{Q_0}\right) C \quad (1)$$

where q_e ($\mathrm{mg\,g^{-1}}$) and C_e ($\mathrm{mg\,l^{-1}}$) are the amounts of adsorbed dye per unit weight of adsorbent and equilibrium dye concentration in solution, respectively. Q_0 ($\mathrm{mg\,g^{-1}}$) is a maximum adsorption capacity of the dye (forming a monolayer) per unit weight of adsorbent. K_L is a constant related to the affinity of the binding sites ($\mathrm{l\,mg^{-1}}$). The essential characteristics of the Langmuir isotherm can be expressed by a separation factor R_L [21], which is defined by the following equation.

$$R_L = \frac{1}{(1 + K_L C_0)} \quad (2)$$

where C_0 ($\mathrm{mg\,l^{-1}}$) is the initial concentration of dye. R_L indicates the nature of the adsorption process to be unfavorable ($R_L > 1$), linear ($R_L = 1$), favorable ($0 < R_L < 1$), and irreversible ($R_L = 0$).

The empirical Freundlich equation was given as follows:

$$\ln q_e = \ln K_f + \left(\frac{1}{n}\right) \ln C_e \quad (3)$$

where K_f and n are constants indicating adsorption capacity and intensity, respectively. The Freundlich adsorption constant, n, should be in a range of 1–10 for beneficial adsorption.

Table 3 showed the Q_0 and K_L values for the Langmuir isotherm, the K_f and n values for the Freundlich isotherm, and the regression coefficients (r^2) obtained from the linear regression equation between the values of C_e/q_e and C_e and $\ln q_e$ and $\ln C_e$, respectively (Fig. 7a and b). For the both dyes, the high regression coefficients for the Langmuir and Freundlich isotherms ($r^2 > 0.97$) indicated that the two models were good fit with the experimental data. But for the RB, it can be seen that the Langmuir model ($r^2 = 0.997$) yields a little better fit than the Freundlich model ($r^2 = 0.987$), in agree with the adsorption of vertigo navy marine and reactive dye on activated carbon [19,22].

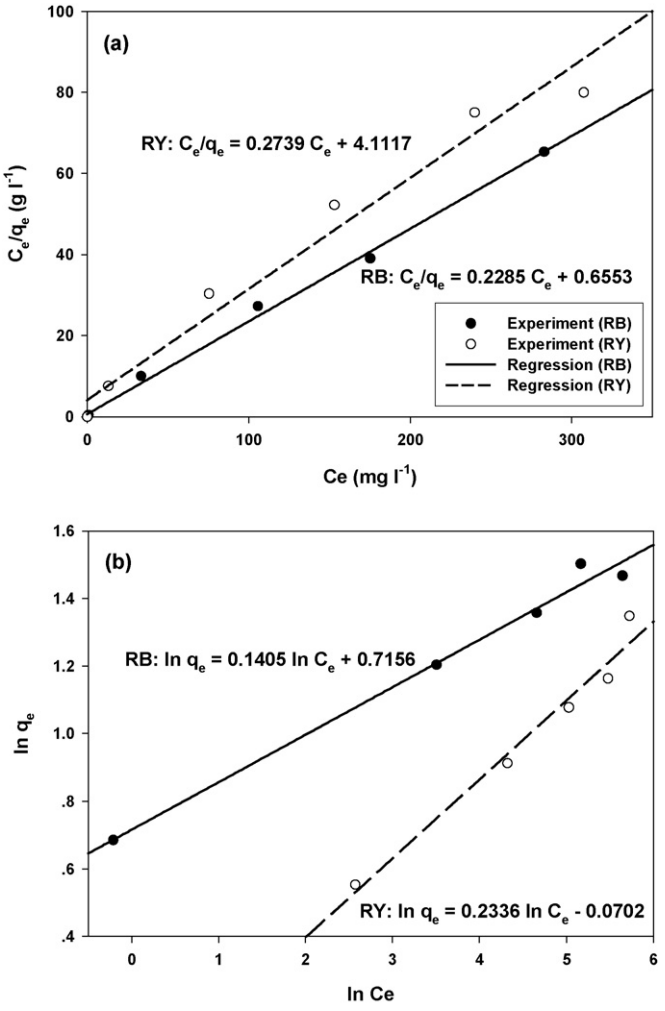

Fig. 7. Langmuir (a) and Freundlich (b) adsorption isotherms of RB and RY on biomass fly ash. Experimental conditions: initial dye concentration range, 10–500 $\mathrm{mg\,l^{-1}}$; fly-ash dose, 2 g/40 ml; contact time, 24 h. Points: experimental data, lines: predicted linear regression models using Langmuir and Freundlich models.

The Q_0 from the Langmuir isotherm indicated that the adsorption capacity of FA-BM was greater for the RB ($4.38\,\mathrm{mg\,g^{-1}}$) than the RY ($3.65\,\mathrm{mg\,g^{-1}}$). The R_L values of the RB and RY were found to be between 0.006 to 0.223 and 0.029 to 0.600 for dye concentrations of 10–500 $\mathrm{mg\,l^{-1}}$, respectively (data not shown). The observed R_L values indicate favorable adsorption of the RB and RY on fly ash ($0 < R_L < 1$).

Table 3
The Q_0 and K_L values for the Langmuir isotherm, the K_f and n values for the Freundlich isotherm and the regression coefficients of equations

Dye	Langmuir			Freundlich		
	Q_0 ($\mathrm{mg\,g^{-1}}$)	K_L ($\mathrm{l\,mg^{-1}}$)	r^2	K_f	n	r^2
Reactive Black 5	4.38	0.349	0.997	2.05	7.12	0.987
Reactive Yellow 176	3.65	0.067	0.972	0.93	4.28	0.971

Table 4
Comparison of the Q_0 for various adsorbents

Dyes	Adsorbent	Q_0 (mg g^{-1})	Reference
Reactive Black 5	Biomass fly ash	4.38	This work
	Coal fly ash (high lime)	7.94	[22]
	Powdered activated carbon	58.8	[22]
	Bagasse fly ash	16.42	[15]
	Modified zeolite	60.6	[8]
	Modified clay (sepiolite)	120.5	[8]
	Brown seaweed (acid treated)	73.2	[10]
	Activated carbon (300–500 μm)	434	[25]
	Activated carbon (500–600 μm)	333	[25]
	Activated carbon (600–700 μm)	278	[25]
Reactive Blue 222	Granular activated carbon (250–2000 μm)	6.53	[7]
	Coal-based bottom ash (>590 μm)	4.02	[7]
Reactive Blue 2	Activated carbon (300–500 μm)	208.8	Recalculated [19]
Reactive Yellow 176	Biomass fly ash	3.65	This work
	Modified zeolite	88.5	[8]
	Modified clay (sepiolite)	169.1	[8]
Reactive Yellow 2	Activated carbon (300–500 μm)	209.4	Recalculated [19]
Reactive Yellow 64	Calcined alunite	236	[16]
Sunset Yellow	Powdered peanut hull	13.99	[2]

Comparison of the Q_0 obtained from this study and other adsorbents was presented in Table 4. The FA-BM gave a similar Q_0 to high lime fly ash [12], coal-based bottom ash, and granular activated carbon [7]. However, the Q_0 obtained from this study was relatively low, when compared to other studies, such as activated carbon and modified sepiolite and zeolite for RB adsorption. Despite relatively low adsorption capacity of the studied fly ash, the use of this adsorbent for dye removal is of interest since it is low-cost and readily available waste.

The K_f from the Freunlich isotherm suggested that the adsorption capacity of FA-BM was greater for the RB than RY. In addition, the n values of the RB and RY were 7.12 and 4.28, indicating favorable adsorption ($1 < n < 10$).

3.6. Effect of contact time

The adsorption of dye on the FA-BM was studied with contact time (Fig. 8a). Adsorption of dye was rapid in the first 30 min, and then the dye adsorption rate gradually increased with contact time until 24 h and subsequently insignificantly changed. The adsorption capacity of the FA-BM was slightly greater for the RB than that of the RY.

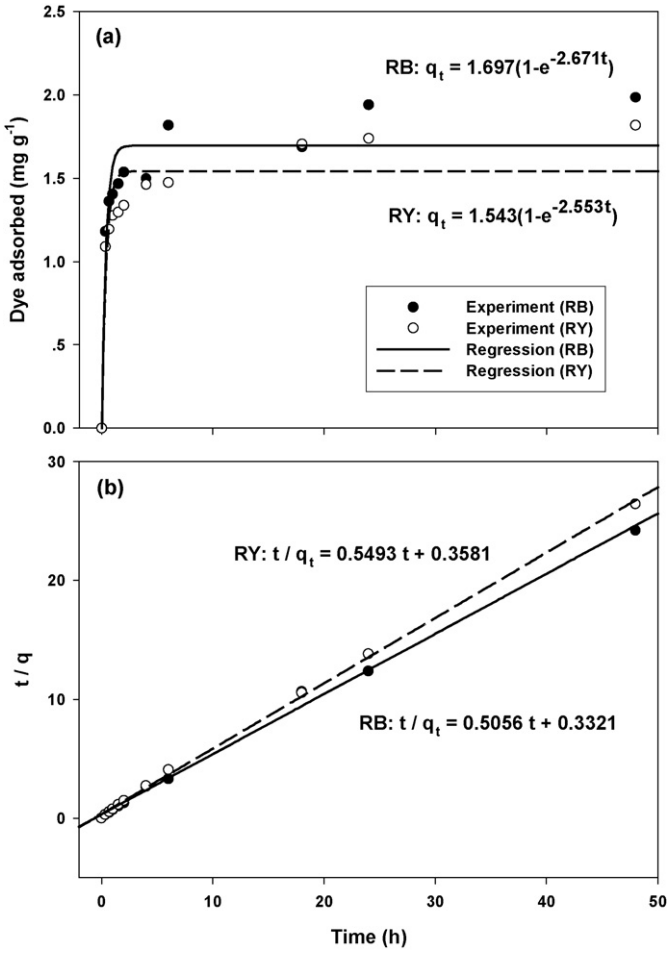

Fig. 8. Lagergren first-order (a) and pseudo-second-order kinetics (b) of RB and RY on biomass fly ash. Experimental conditions: initial dye concentration range, 100 mg l^{-1}; fly-ash dose, 2 g/40 ml. Points: experimental data, lines: predicted non-linear and linear regression models using Lagergren first-order and pseudo-second-order model, respectively.

3.7. Adsorption kinetics

In this study, the kinetic data of the FA-BM were analyzed using the Lagergren first-order and pseudo-second-order rate equations. These equations have been used widely for the adsorption of an adsorbate from an aqueous solution. The best fit model was considered based on the regression coefficient (r^2) and the experimental q_e.

3.7.1. First-order kinetic model

The Lagergren first-order was defined as follows [23]:

$$\log(q_e - q_t) = \log q_e - \frac{k_1 t}{2.303} \quad (4)$$

where q_e and q_t are the amount of dye adsorbed per unit weight of the adsorbent (mg g^{-1}) at equilibrium time and time t, respectively. k_1 is the rate constant for the first-order kinetics. For the Lagergren first-order rate equation, it is better to apply the following equation to avoid the unknown q_e.

$$q_t = q_e(1 - e^{-k_1 t}) \quad (5)$$

Table 5
Lagergren first-order and pseudo-second-order adsorption rate constants and the calculated ($q_{e,cal}$) and experimental q_e ($q_{e,exp}$) at initial dye concentration of 100 mg l^{-1}

Dye	$q_{e,exp}$ (mg g^{-1})	Pseudo-first-order kinetic model			Pseudo-second-order kinetic model		
		$q_{e,cal}$ (mg g^{-1})	k_1 (h^{-1})	r^2	$q_{e,cal}$ (mg g^{-1})	k_2 (g mg^{-1} h^{-1})	r^2
Reactive Black 5	1.94	1.70	2.67	0.888	1.98	0.770	0.997
Reactive Yellow 176	1.74	1.54	2.55	0.875	1.82	0.843	0.999

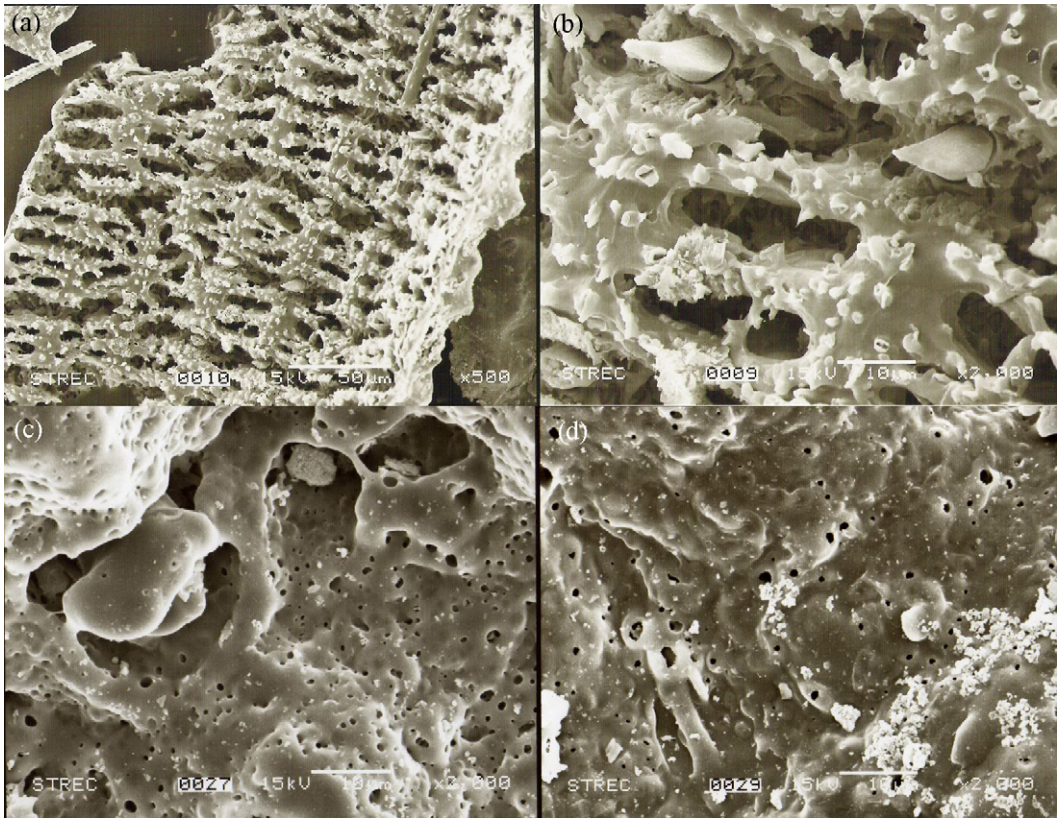

Fig. 9. SEM images of the biomass fly ash before (a and b) and after adsorbing the RB (c) and RY (d).

Fig. 8a and Table 5 showed the rate constant, calculated q_e, and regression coefficient of the first-order kinetic model. Based on regression coefficient ($r^2 < 0.89$), it appeared that the first-order model was not well fit with the experimental data. In addition, the q_e from the calculation was different from the experimental q_e (Table 5).

3.7.2. Pseudo-second-order kinetic model

The pseudo-second-order rate equation was defined as follows [24]:

$$\frac{t}{q_t} = \frac{1}{k_2 q_e^2} + \frac{t}{q_e} \quad (6)$$

where k_2 is the rate constant for the second-order kinetics.

Fig. 8b and Table 5 showed the sorption kinetics of dyes and rate constants obtained from the pseudo-second-order kinetic model. The sorption data was good fit with the pseudo-second-order kinetic model. The regression coefficients of the second-order model ($r^2 > 0.99$) were greater than that of the first-order model for both dyes. The results also showed the experimental and calculated values of q_e agreed with each other (Table 5). Therefore, the adsorption process of the studied dyes onto the FA-BM could be better explained by the pseudo-second-order model than the first-order kinetic model. Based on the pseudo-second-order model, these observations indicate that the rate of dye adsorption process is controlled by the chemisorption process [18,22], which is depended on the chemical character of FA-BM and dyes [12]. Similar kinetic results were also found in the sorption of Brilliant Green on rice husk ash [3], in the sorption of Direct Blue 71 on palm ash [18], and in the sorption of RB on high lime coal fly ash [22].

3.8. SEM images

The SEM images of FA-BM before and after dye adsorption were shown in Fig. 9. The FA-BM had a net-like structure and macropores. After adsorption of both RB and RY, the surface

and pores of FA-BM were coated with dyes causing smoother surface and minimizing pore size.

4. Conclusions

Results of this study provide for a better understanding of the adsorption behavior of reactive dyes on biomass fly ash. Among the studied fly ashes, the biomass fly ash was the best adsorbent of dyes. The adsorption pattern of both dyes on the biomass fly ash was pH-dependent with a maximum adsorption capacity at the final pH of 8.1–8.5. The addition of salt had a positive effect on the adsorption capacity of the biomass fly ash. An increase in the initial dye concentration enhances the interaction between dye and biomass fly ash, resulting in greater adsorption capacity. The equilibrium data of both dyes were fitted to both Langmuir and Freundlich isotherms. The monolayer adsorption capacity of the biomass fly ash was found to be greater for the Reactive Black 5 (4.38 mg g^{-1}) than the Reactive Yellow 176 (3.65 mg g^{-1}). The adsorption process conformed to the second-order kinetic model. Overall, the studied biomass fly ash showed a potential application as adsorbent for reactive dye wastewater.

Acknowledgements

We wish to acknowledge the funding by the Thai Research Fund and the Faculty of Science, Kasetsart University (ScRF) for supporting this research. Thanks also to Pattarawan Chularuengoaksorn, Nichada Chatsatapattayakul, and Saowalak Sirijareontanapun, for their technical support.

References

[1] S.K. Alpat, O. Ozbayrak, S. Alpat, H. Akcay, The adsorption kinetics and removal of cationic dye, Toluidine Blue O, from aqueous solution with Turkish zeolite, J. Hazard. Mater. 151 (2008) 213–220.
[2] R. Gong, Y. Ding, M. Li, C. Yang, H. Liu, Y. Sun, Utilization of powdered peanut hull as biosorbent for removal of anionic dyes from aqueous solution, Dyes Pigments 64 (2005) 187–192.
[3] V.S. Mane, I.D. Mall, V.C. Srivastava, Kinetic and equilibrium isotherm studies for the adsorptive removal of Brilliant Green dye from aqueous solution by rice husk ash, J. Environ. Manage. 84 (2007) 390–400.
[4] V. Ponnusami, V. Kritika, R. Madhuram, S.N. Srivastava, Biosorption of reactive dye using acid-treated rice husk: factorial design analysis, J. Hazard. Mater. 142 (2007) 397–403.
[5] P. Janos, H. Buchtova, M. Ryznarova, Sorption of dyes from aqueous solutions onto fly ash, Water Res. 37 (2003) 4938–4944.
[6] A. Aguedach, S. Brosillon, J. Morvan, E.K. Lhadi, Photocatalytic degradation of azo-dyes Reactive Black 5 and Reactive Yellow 145 in water over a newly deposited titanium dioxide, Appl. Catal. B 57 (2005) 55–62.
[7] A.R. Dincer, Y. Gunes, N. Karakaya, E. Gunes, Comparison of activated carbon and bottom ash for removal of reactive dye from aqueous solution, Bioresource Technol. 98 (2007) 834–839.
[8] O. Ozdemir, B. Armagan, M. Turan, M.S. Celik, Comparison of the adsorption characteristics of azo-reactive dyes on mezoporous minerals, Dyes Pigments 62 (2004) 49–60.
[9] M.F.R. Pereira, S.F. Soares, J.J.M. Orfao, J.L. Figueiredo, Adsorption of dyes on activated carbons: influence of surface chemical groups, Carbon 41 (2003) 811–821.
[10] K. Vijayaraghavan, Y.-S. Yun, Biosorption of C.I. Reactive Black 5 from aqueous solution using acid-treated biomass of brown seaweed *Laminaria sp.*, Dyes Pigments 76 (2008) 726–732.
[11] A. Bousher, X. Shen, R.G.J. Edyvean, Removal of coloured organic matter by adsorption onto low-cost waste materials, Water Res. 31 (1997) 2084–2092.
[12] Z. Eren, F.N. Acar, Equilibrium and kinetic mechanism for Reactive Black 5 onto high lime Soma fly ash, J. Hazard. Mater. 143 (2007) 226–232.
[13] P.C.C. Faria, J.J.M. Orfao, M.F.R. Pereira, Adsorption of anionic and cationic dyes on activated carbons with different surface chemistries, Water. Res. 38 (2004) 2043–2052.
[14] S. Wang, Z.H. Zhu, Sonochemical treatment of fly ash for dye removal from wastewater, J. Hazard. Mater. B 126 (2005) 91–95.
[15] M. Rachakornkij, S. Ruangchuay, S. Teachakulwiroj, Removal of reactive dyes from aqueous solution using bagasse fly ash, Songklanakarin J. Sci. Technol. 26 (Suppl. 1) (2004) 13–24 (in Thai).
[16] M. Ozacar, I.A. Sengil, Adsorption of reactive dyes on calcined alunite from aqueous solution, J. Hazard. Mater. 98 (2003) 211–224.
[17] E.E. Hughes, D.A. Tillman, Biomass cofiring: status and prospects 1996, Fuel Process. Technol. 54 (1998) 127–142.
[18] A.A. Ahmad, B.H. Hameed, N. Aziz, Adsorption of direct dye on palm ash: kinetic and equilibrium modeling, J. Hazard. Mater. 141 (2007) 70–76.
[19] Y.S. Al-Degs, M.I. El-Barghouthi, A.H. El-Sheikh, G.M. Walker, Effect of solution pH, ionic strength, and temperature on adsorption behavior of reactive dyes on activated carbon, Dyes Pigments 77 (2008) 16–23.
[20] D.L. Sparks, Environmental soil chemistry, Academic Press, USA, 1995.
[21] K.R. Hall, L.C. Eagleton, A. Acrivos, T. Vermeulen, Pore-and-solid-diffusion kinetics in fixed-bed absorption under constant-pattern conditions, Ind. Eng. Chem. Fund. 5 (1996) 212–223.
[22] Z. Eren, F.N. Acar, Adsorption of Reactive Black 5 from an aqueous solution: equilibrium and kinetic studies, Desalination 194 (2006) 1–10.
[23] S. Lagergren, Zur theorie der sogenannten adsorption geloster stafe, Kungliga Svenska Vetenskapsakademiens, Handlingar 24 (1898) 1–39.
[24] G. Blanchard, M. Maunaye, G. Martin, Removal of heavy metals from waters by means of natural zeolites, Water Res. 18 (1984) 1501–1507.
[25] Y. Al-Degs, M. Khraisheh, S. Allen, M. Ahmad, Effect of carbon surface chemistry on the removal of reactive dyes from textile effluents, Water Res. 34 (2000) 927–935.